Journal of Catalysis **196,** 174–179 (2000)
doi:10.1006/jcat.2000.3021, available online at http://www.idealibrary.com on IDEAL®

Inelastic Neutron Scattering Investigation of the Nature of Surface Sites Occupied by Hydrogen on Highly Dispersed Platinum on Commercial Carbon Black Supports

Peter Albers,*,[1] Emmanuel Auer,† Karsten Ruth,‡ and Stewart F. Parker§

*Degussa-Hüls Group, Department of Physical Chemistry, IR-ATS-PCP, Infracor GmbH, P.O. Box 1345, D-63403 Hanau, Germany; †Sivento Division, Chemical Catalysts and Zeolites, Degussa-Huels AG, P.O. Box 1345, D-63403 Hanau,Germany; ‡Fuel Cell Division, Degussa Metals Catalysts Cerdec AG, dmc^2, P.O. Box 1351, D-63403 Hanau, Germany; and §Rutherford Appleton Laboratory, ISIS Facility, Chilton, Didcot, Oxfordshire, OX11 0QX, UK

Received May 19, 2000; revised June 29, 2000; accepted July 3, 2000

It is shown that inelastic neutron scattering is uniquely suitable to study the surface sites occupied by atomic hydrogen at the surfaces of 2–4-nm platinum particles on hydrogen-containing, high-surface-area carbonaceous support materials. Molecular and atomic hydrogen species can be discriminated under 800–1200 mbar of hydrogen pressure relevant for the operation conditions of fuel cells and other platinum-based catalysts. The distribution of sites suggests that the shape of the particles is intermediate between cubic and cuboctahedral. © 2000 Academic Press

Key Words: **platinum; carbon black; hydrogen; fuel cell catalysts; inelastic neutron scattering; INS.**

INTRODUCTION

Platinum and supported platinum metal and alloy catalysts are commonly used in various chemical processes. Some typical large-scale applications of Pt-based catalyst technology are the synthesis of HCN from methane and ammonia (1), the oxidation of ammonia for the production of nitric acid (2), and exhaust gas purification processes (3). Furthermore, for the production of fine chemicals, pharmaceuticals, or agrochemicals, supported platinum catalysts are used in the various types of hydrogenation or oxidation reactions (4, 5). Due to the technological importance of this precious metal, the interdependencies between the physical/chemical properties of platinum surfaces and the catalytic properties have been studied under many different conditions and are well documented in detail (6, 7 and literature cited therein).

A prominent and steadily growing field of application is the use of platinum (or one of its alloys) supported on electrically conducting carbons, preferably carbon blacks. These are used as highly platinum-loaded electrocatalysts in fuel cell applications. In the field of low-temperature fuel cells, e.g., phosphoric acid fuel cells (PAFC), proton exchange membrane fuel cells (PEMFC), and direct methanol fuel cells (DMFC), carbon black-supported catalysts are considered to be the most promising electrocatalytic materials for the conversion of hydrogen and oxygen into water, electrical power, and heat (8, 9).

As described by Kinoshita (10), the particle size of the precious metal affects many properties. In particular, the oxygen reduction kinetics in acid electrolytes are structure sensitive. This aspect has the dominant influence on the oxygen mass activity in PEMFC and PAFC. Therefore, a more detailed identification of structural/geometrical requirements of certain surface sites as well as the generation of active sites by adequate catalyst preparation techniques is of importance for improving catalyst performance.

In fuel cell applications high precious metal loadings are preferable but a sufficiently low particle size is also essential. The interactions between the catalyst and protons under realistic operating conditions are of paramount interest. Unfortunately, surface analysis techniques for directly studying the interactions between hydrogen and finely divided platinum particles on the high-surface-area, partly porous carbonaceous supports typically used in fuel cell applications seem quite limited. The small precious metal particles as well as the finely divided carbon blacks which are used for fuel cell applications absorb electromagnetic radiation from the infrared through the visible. As a result, the full analytical power of well-established techniques such as Raman spectroscopy, using either visible or near-infrared excitation, and infrared spectroscopy including reflection–absorption infrared techniques cannot be utilized. The application of nuclear magnetic resonance techniques is seriously limited by the electrical conductivity of the carbon blacks.

Furthermore, for investigating these platinum-based fuel cell catalysts, surface analytical techniques are essential

---

[1] To whom correspondence should be addressed. E-mail: peter.albers@infracor.de or peter.albers@degussa-huels.de.

0021-9517/00 $35.00

which allow the characterisation of the catalyst surfaces under *in situ* conditions.

Recent studies have shown that inelastic incoherent neutron scattering (INS) is uniquely able to reveal micromorphological features of carbon blacks (11) used as supports in catalyst applications (12). Even closely related materials show significant differences and surface properties of carbon blacks may be successfully monitored under the original as well as the graphitized conditions. Further, as shown by Renouprez and Jobic (13), INS is an excellent method with which to study hydrogen on Pt/SiO_2 catalysts.

In the present paper the potential of *in situ* INS for investigating the interactions between gaseous hydrogen and the surfaces of platinum particles of about 2–4 nm size supported on finely divided hydrogen-containing carbon blacks is demonstrated.

EXPERIMENTAL

The platinum catalysts of 20 wt.% and of 40 wt.% precious metal loading on carbon black were prepared according to the usual wet impregnation procedure well documented in the literature (see, e.g., 14, 15). As support material a furnace black with a BET surface area of 254 m^2/g was used. The hydrogen content of the carbon black was determined by use of an LECO-RH-404 hydrogen analyser as 2030 ± 200 ppm.

Transmission electron microscopy together with statistical evaluations of the particle size distributions obtained (evaluation of 4000 particles per sample) revealed an average primary particle size of the precious metal of 2.2 nm on the 20% and 3.9 nm on the 40% catalyst.

The catalysts were sealed into thin-walled aluminum (99.99%) cells which were evacuated to 10^{-5} mbar and closed by means of welded bellow valves (Nupro). Afterward a catalyst was slowly exposed to hydrogen (99.999% Messer-Griesheim) at 22°C in steps of a few millibar each over several days using a gas volumetric device including capacitive pressure transducers (MKS Baratron). The adsorption was controlled such that a pronounced macroscopic heating of the catalyst powder due to the heat of adsorption was avoided during the H_2/Pt interactions. In the first step, the pressure in the can was limited to 100 mbar. Afterward the can was pumped out again ending with the vacuum of the turbomolecular pump. The procedure was repeated in a second hydrogenation cycle ending with 300 mbar. Afterward the hydrogenation/dehydrogenation cycle was repeated three times ending with 1.5 bar each. This procedure was chosen to carefully remove residual amounts of oxygen, water, and volatile organic species from the catalysts surface and to activate the surface for controlled hydrogen uptake. The adsorption activity of the catalysts to hydrogen was monitored by gas volumetric methods.

After removal of the hydrogen in a final step the cans were loaded to the final equilibrium pressures noted in the figures and sealed in the aluminum cans prior to the *in situ* INS experiment.

Using the gas volumetric values as monitored during careful and stepwise hydrogen dosing the H consumption by the precious metal was calculated. (H stands for atomic hydrogen assuming predominantly and efficiently dissociative adsorption; this is confirmed by the results in the following section.) H/Pt values of about 0.41 were obtained for the 20% Pt sample at a hydrogen equilibrium pressure of 1.2 bar. This sample contains platinum particles of smaller size. For the 40% Pt sample at 0.8 bar the H/Pt value was about 0.12 which is in line with the lower equilibrium pressure adjusted and the significantly higher particle size of the supported platinum entities in this sample.

INS spectra were recorded at 20 K using the TOSCA (16) spectrometer at the spallation neutron source ISIS (Rutherford Appleton Laboratory, UK).

After measurement of the original catalysts under hydrogen, the cans were pumped down to the vacuum of a turbomolecular pump. Subsequently, the INS spectra of the Pt/C catalysts were recorded to differentiate between the scattering of the hydrogenous species at the catalyst surface and the hydrogenous scattering of the carbon black support containing chemically bound hydrogen.

RESULTS AND DISCUSSION

Figures 1 and 2 show the INS spectra of the Pt(20%)/C and Pt(40%)/C catalysts at 20 K. Figures 1a and 2a are those with adsorbed hydrogen, Figs. 1b and 2b show the spectra of the corresponding sample at 20 K after evacuation at room temperature, and Figs. 1c and 2c show the difference spectra. All of the features in Figs. 1c and 2c are

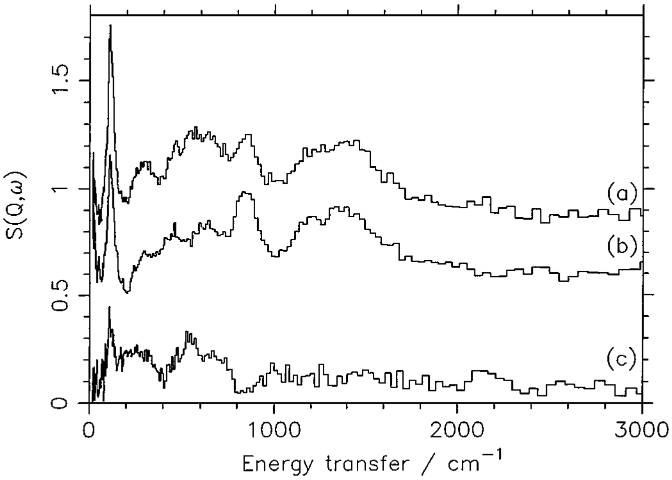

FIG. 1. INS spectra of (a) the Pt(20%)/C catalyst under 1.2 bar H_2 gas, (b) after evacuation, and (c) the difference spectrum (a)–(b).

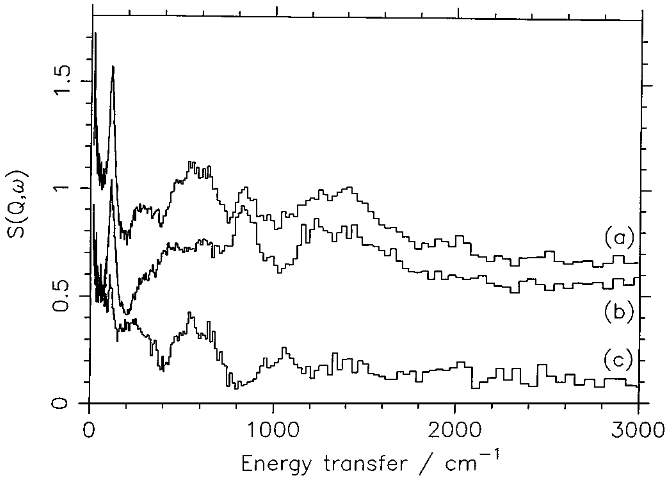

FIG. 2. INS spectra of (a) the Pt(40%)/C catalyst under 0.8 bar H_2 gas, (b) after evacuation, and (c) the difference spectrum (a)–(b).

assigned to hydrogen bound to the metal or to physisorbed H_2. Hydrogen covalently bound to the carbon is unaffected by evacuation as evidenced by the bands at 825 cm^{-1} in Figs. 1b and 2b. Previous work (11) has shown that these are due to hydrogen attached to the aromatic rings of the graphitic network. In addition, there are no enhanced contributions of polyaromatic species indicative of pronounced hydrogasification of the support material as was detected by INS of Pd/activated carbon catalysts (12). The difference spectra show that the out-of-plane and the in-plane bending modes of terminating hydrogen species predominantly located at the edges of the basic structural units of the carbonaceous support are well separated from the hydrogenous scattering from molecular and atomic hydrogen. This suggests the feasabiliy of related studies on platinum catalysts based on graphitized carbon blacks as well as on furnace blacks of higher hydrogen content whose INS spectra are shown in (11). An essential point is that the material has to be dry (11).

In Figs. 1a and 2a, the graphite band at ~110 cm^{-1} is asymmetrically broadened due to overlap with the $J=0$ to $J=1$ rotational transition of molecular H_2. This is more clearly seen in the difference spectra where the transition at 120 cm^{-1} and the broad recoil feature (centered at 250 cm^{-1}) associated with it are evident. The similarity to solid hydrogen (17) indicates that the molecular H_2 is physisorbed across the catalyst surface, as was seen for a Ru/C catalyst (18).

If only the topmost layer of metal atoms is considered, four types of hydrogen adsorption sites are available. These are the on-top, two-, three-, and fourfold bridge sites which involve hydrogen coordinated to one, two, three, and four metal atoms, respectively. Each site gives rise to a totally symmetric mode which involves motion perpendicular to the surface and to two other modes that involve motion parallel to the surface. For the on-top site, the bending mode is degenerate if the local symmetry includes either a C_3 or C_4 axis perpendicular to the surface; for lower symmetries the mode splits. For simplicity, we will assume that the local symmetry is C_{3v}, i.e., a (111) surface, but the same results are obtained if a C_{4v} (100) surface is considered. This seems to be the only suitable way to proceed without introducing extra bands. For the two-, three-, and fourfold cases C_{2v}, C_{3v}, and C_{4v} symmetries are assumed; the latter two have twofold degenerate parallel modes.

For the on-top site the Pt–H stretch has been observed at about 2120 cm^{-1} on Pt(16.3%)/SiO_2 (19) and on EUROPT1 (Pt(6%)/SiO_2) (20). The bending frequency is unknown; however, in metal complexes the vibration is usually in the range 600–800 cm^{-1} (21). The INS spectrum of $HCo(CO)_4$ has an intense band at 696 cm^{-1} assigned to this mode (22). For the present work, we will use a value of 650 cm^{-1} for this mode.

For the twofold C_{2v} bridge site three modes are expected: A_1, B_1, and B_2. The best-characterised system is hydrogen on W(100). The frequency of the symmetric stretch mode is coverage dependent and the frequency is believed to be a direct measure of the W–W distance. At saturation there are two H atoms per tungsten atom and the three modes are at 1050 cm^{-1} (A_1), 1290 cm^{-1} (B_1), and 635 cm^{-1} (B_2) (23, 24). On the Pt(100)–(1 × 1) surface, adsorption of hydrogen produces one new band that is coverage dependent in the range 1190–1230 cm^{-1} (25) assigned to the symmetric mode of the twofold bridge. (The hydrogen in the fourfold hollow site is considered to be shielded by the surrounding metal atoms and so is unobservable.) Using a Pt–Pt distance of 2.8 Å, a Pt–H distance of 1.8 Å, and a simple valence bond model the asymmetric stretch mode is predicted to be at 1400 cm^{-1}. Since the stretching modes are 10% higher in energy on platinum than on tungsten, we will assume that the bending mode may also be up to 10% higher, i.e., near 700 cm^{-1}.

For the threefold C_{3v} bridge site only two modes are expected (of A_1 and E symmetry). The literature is confusing. Electron energy loss spectroscopy of hydrogen on Pt(111) shows two intense losses at 550 and 1250 cm^{-1} with a weaker feature at ~860 cm^{-1} (26, 27). Low-energy recoil scattering of rare gas ions shows that only the face-centred threefold hollow site (i.e., there is platinum atom directly below in the second layer) is occupied (28). Thus one of the modes must be due to a surface contaminant. Infrared spectroscopy (29) of the same system shows one band at 1254 cm^{-1}; from the metal surface selection rule, this must be a totally symmetric mode. Theory predicts the A_1 mode at 1339 cm^{-1} (30) and 1192–1210 cm^{-1} (31) in reasonable agreement with the infrared measurement. The E mode is predicted (30) to be at 919 cm^{-1}; however, the fact that the 550 and 1250 cm^{-1} bands grow in together in the EELS experiments strongly suggests that they belong to the same species, and hence the

550 cm^{-1} band is assigned to the E mode and the 860 cm^{-1} to a contaminant.

The fourfold C_{4v} bridge site is characterised by two modes (of A_1 and E symmetry). These are expected to be at low frequency. On Rh(100) two vibrations are found at 660 and 532 cm^{-1} (32) assigned as A_1 and E, respectively, and on Pd(100) bands at 510 and 613 cm^{-1} (33) are assigned as E and A_1, respectively. For a threefold site, it was argued (30) that the hydrogen–substrate bond strength is determined not just by coordination to specific atoms but also by interaction with the delocalized metal electrons. The effect of this is to increase the restoring force perpendicular to the surface and hence the frequency of the totally symmetric mode. Since for a fourfold site, the hydrogen is even more "buried" in the surface, the same argument presumably holds true. Thus we assign for both Rh(100) and Pd(100) the lower energy mode to the asymmetric stretch and the higher energy mode to the symmetric stretch. Further, as the frequencies of each mode are so similar on both surfaces, we will assume that on the platinum particles the E mode is near 500 cm^{-1} and the A_1 mode is near 650 cm^{-1}.

One of the advantages of INS spectroscopy is that it makes it possible to model both the frequencies and intensities from a conventional normal coordinate analysis (34). We have assumed that the Pt–H bond length is 1.8 Å and the Pt–Pt distance is 2.8 Å. For all of the sites considered here, since it is the intensities that are the relevant quantity, minor (±20%) variations in the Pt–H and Pt–Pt distance can be easily accommodated by varying the force constants, without causing large changes in the calculated intensity. Thus the results are not sensitive to the choice of these parameters; the important factor is the symmetry. Using the frequencies given above, each adsorption site can be modeled using the program CLIMAX (35) and the results are shown in Fig. 3. An important difference between INS spectroscopy and infrared and Raman spectroscopies is that overtones and combinations are allowed transitions in the harmonic approximation and may have significant intensities. Figures 3b–3e include the contributions from the binary combinations and first overtones for each site and show that their contribution to the total intensity must be considered. Table 1 gives the frequencies of each site.

The calculated spectra are a convolution of a delta function with the instrument resolution function and are much narrower than the experimental bands. There are two reasonable possibilities for this. First, the metal particles are not of uniform size so the width of the bands reflects the inhomogeneities of the system and different sites are occupied. Second, coupling between adjacent oscillators can occur giving rise to dispersion in the mode. Since INS is sensitive to all wavevectors, the dispersion gives rise to band broadening. The other result of dispersion is that it can give rise to complex bandshapes with submaxima that could be assigned as modes of a different species. This is commonly seen in hydrogen-in-metal systems (36). The INS spectrum of hydrogen adsorbed on platinum black (37) has a bandshape that is not dissimilar to that observed here and in this case dispersion has been shown to be the cause. However, the average particle size of the platinum black, 12 nm, was much larger than that used here, 2 and 4 nm for the 20% and 40% Pt catalysts, respectively. The larger particles would mean that the extended networks needed for dispersion would be more easily formed. In addition, Renouprez and Jobic (13) have shown that on EUROPT1 (which also has small particles), the bandshape does not change with coverage, suggesting that dispersion is not important for the supported catalysts. Nonetheless, it must be recognised that if significant dispersion is present, then the arguments below about the type of sites present may not be valid.

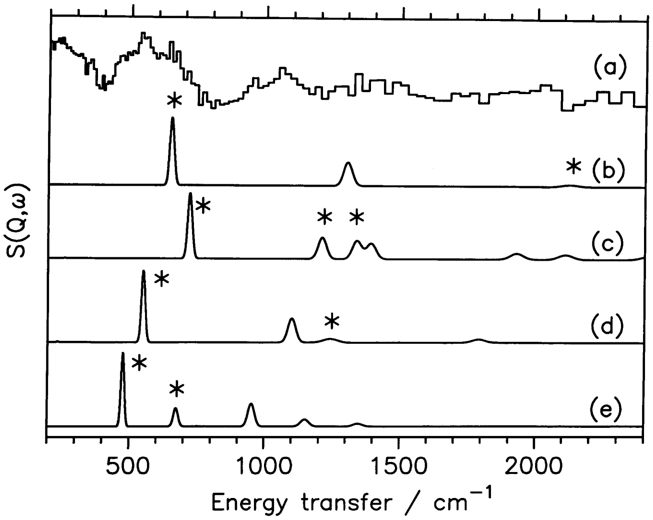

FIG. 3. (a) Difference spectrum of the Pt(40%)/C catalyst and simulated INS spectra of (b) the on-top site in C_{3v} symmetry, (c) the twofold bridge site in C_{2v} symmetry, (d) the threefold bridge site in C_{3v} symmetry, and (e) the fourfold bridge site in C_{4v} symmetry. The fundamentals are marked by asterisks.

TABLE 1

Frequencies of Each Site

Site	Symmetry	Frequency (cm^{-1})	Description
On-top	C_{3v}	2125	Stretch (A_1)
		650	Bend (E)
Twofold bridge	C_{2v}	1400	Asymmetric stretch (B_1)
		1200	Symmetric stretch (A_1)
		720	Out-of-plane bend (B_2)
Threefold bridge	C_{3v}	1360	Symmetric stretch (A_1)
		550	Asymmetric stretch (E)
Fourfold bridge	C_{4v}	650	Symmetric stretch (A_1)
		550	Asymmetric stretch (E)

Curvefitting the region 400–800 cm^{-1} of the spectra in Figs. 1c and 2c to a sum of Gaussian peaks shows that there are a minimum of four peaks present at 470, 550, 650, and 720 cm^{-1}. The work on metal single crystals has clearly shown that the most stable sites are those of high coordination number. On frequency and intensity grounds, the peaks at 470 and 550 cm^{-1} are assigned to the E modes of the fourfold and threefold sites, respectively. The 650 cm^{-1} peak is too strong to be solely due to the A_1 mode of the fourfold site (the intensity ratio $E:A_1$ is ~3 : 1, see Fig. 3e), and it is assigned to the bending mode of the on-top species. (The presence of a substantial quantity of the on-top species is justified later.) The remaining feature at 720 cm^{-1} could be either the A_1 mode of the fourfold site or the out-of-plane B_2 mode of the twofold site. The frequency is at the extreme for both species; however, the work (24) on Pt(100) shows that both twofold and fourfold sites are occupied on the (100) face, so we assign the 720 cm^{-1} band to the twofold species.

Figure 4 shows the difference spectra of the Pt(20%)/C and Pt(40%)/C catalysts and the fits using the peak positions given in Table 1 and a linewidth of 80 cm^{-1}. In both cases the intensity in the region above 1400 cm^{-1} is underestimated. In this region second overtones and ternary combinations occur and these are not calculated in CLIMAX.

Table 2 shows the percentage of each species present for the two catalysts. It is apparent that the distribution is similar for both catalysts. In neither case does it match that expected for a cuboctahedron (10): the quantity of fourfold sites is larger than predicted, suggesting that the particles are intermediate between cubic and cuboctahedral forms. This conclusion depends only on the assignment of the 470 and 550 cm^{-1} bands to the E modes of the threefold and fourfold sites, which are the most reliable assignments.

^1H NMR of EUROPT1 (38) has shown that at 0.7 bar hydrogen pressure ~30% of the hydrogen is present in the on-top site. This is consistent with the infrared measurements (19, 20) that show that the site is only populated with $H_2(g)$ present and that the quantity is pressure dependent. The present results are consistent with this: while the sample cans were charged to 0.8 (40% catalyst) and 1.2 bar (20% catalyst) at room temperature, the measurement was carried out at 20 K so the pressure in the can would have been markedly reduced, accounting for the difference between the NMR results and the present work. The present results show that the intensity in the 2100 cm^{-1} region is mainly due to overtones and combinations of the multiply bonded hydrogen species and only a minor proportion is due to the on-top site.

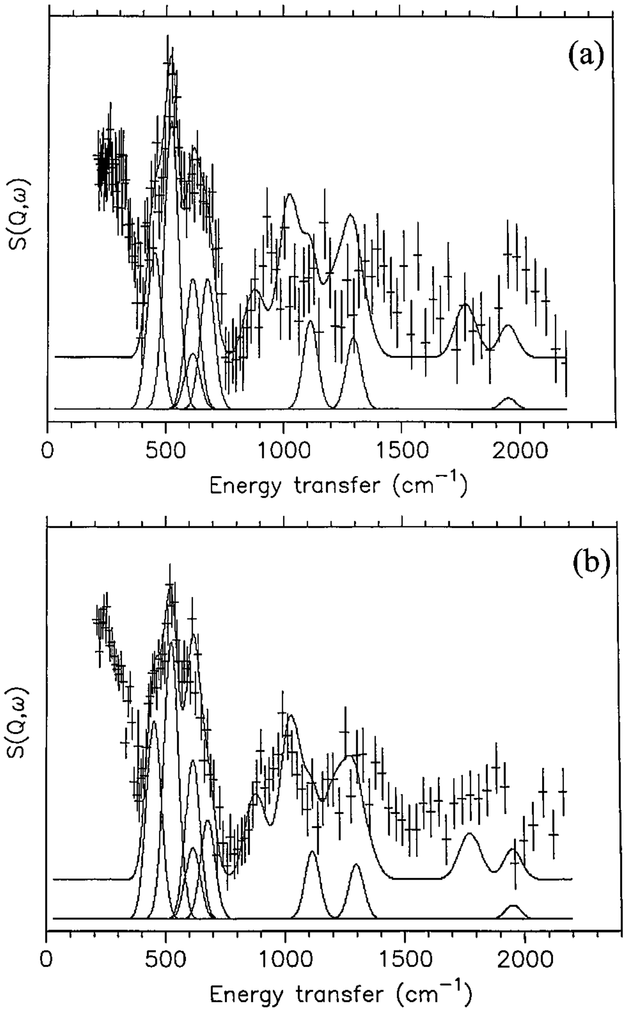

FIG. 4. Difference INS spectra of the catalysts (crosses) and fits as a sum of components (solid line). (a) Pt(20%)/C; (b) Pt(40%)/C. The fundamentals are shown as individual Gaussians, and the remaining intensity is due to first overtones and binary combinations.

TABLE 2

Proportions (%) of Each Type of Site Present on the Catalysts

Site	Pt(20%)/C	Pt(40%)/C
On-top	16	19
Twofold bridge	29	22
Threefold bridge	34	33
Fourfold bridge	21	26

EUROPT1 is made by a similar route to the present materials (reduction of hexachloroplatinic acid) but with a different support (SiO_2 instead of carbon). The spectra and conclusions from the earlier study (10) are in general agreement with the present work. This suggests that in the absence of strong metal–support interaction, the support exerts only a minor influence on the crystal form.

CONCLUSIONS

It is shown that inelastic neutron scattering is uniquely able to study the surface sites occupied by atomic hydrogen at the surfaces of 2–4-nm platinum particles on hydrogen-containing, high-surface-area carbonaceous support materials. Molecular and atomic hydrogen species can be discriminated under 800–1200 mbar hydrogen pressure relevant for the operation conditions of fuel cells and other platinum-based catalysts.

These results are of direct practical relevance since they demonstrate a broad field of opportunities for the INS technique in studying fuel cell catalysts under *in situ* conditions under varying hydrogen pressures and temperatures which are relevant for stationary and nonstationary applications.

Due to the specific physical properties of fuel cell catalysts—low particle size of the precious metal component, finely divided and electrically conductive carbon black supports with high absorption of electromagnetic radiation—results obtained from the INS spectra are not accessible by any other method.

The distribution of sites suggests that the shape of the particles is intermediate between cubic and cuboctahedral.

ACKNOWLEDGMENTS

The Rutherford Appleton Laboratory (UK) is thanked for access to neutron beam facilities.

REFERENCES

1. Klenk, H., Griffiths, A., Huthmacher, K., Itzel, H., Knorre, H., Voigt, C., and Weiberg, O., *in* "Ullmann's Encyclopedia of Industrial Chemistry" (W. Gerhartz, Y. Yamamoto, F. T. Campbell, R. Pfefferkorn, and J. F. Rounsaville, Eds.), Vol. A8, 5th ed., pp. 159–163. VCH, Weinheim, 1987.
2. Thiemann, M., Scheibler, E., and Wiegand, K. W., *in* "Ullmann's Encyclopedia of Industrial Chemistry" (W. Gerhartz, Y. Yamamoto, F. T. Campbell, R. Pfefferkorn, and J. F. Rounsaville, Eds.), Vol. A17, 5th ed., pp. 293–339. VCH, Weinheim, 1987.
3. Taylor, K. C., *in* "Catalysis—Science and Technology" (J. R. Anderson and M. Boudart, Eds.), p. 140. Springer, Berlin, 1984; Kreuzer, T., Lox, E. S., Lindner, D., and Leyrer, J., *Catal. Today* **29**, 17 (1996).
4. Rylander, P., "Catalytic Hydrogenation in Organic Synthesis." Academic Press, New York, 1979.
5. Auer, E., Freund, A., Pietsch, J., and Tacke, T., *Appl. Catal. A: General* **173**, 259 (1998).
6. Somorjai, G. A., "Introduction to surface chemistry and catalysis," pp. 500–525 and literature cited therein. Wiley, New York, 1994.
7. "Hydrogen Effects in Catalysis" (Z. Paal and P. G. Menon, Eds.), and literature cited therein. Dekker, New York, 1988.
8. Grove, W. R., *Philos. Mag.* **86**(14), 127 (1839).
9. Acres, G. J., Frost, J. C., Hards, G. A., Potter, R. J., Ralph, T. R., Thompsett, D., Burstein, G. T., and Hutchings, G. J., *Catal. Today* **38**, 393 (1997).
10. Kinoshita, K., *J. Electrochem. Soc.* **137**, 845 (1990).
11. Albers, P., Prescher, G., Seibold, K., Ross, D. K., and Fillaux, F., *Carbon* **34**, 903 (1996). Albers, P., Seibold, K., Prescher, G., Parker, S. F., Tomkinson, J., Ross, D. K., and Fillaux, F., *Carbon* **37**, 437 (1999).
12. Albers, P., Burmeister, R., Seibold, K., Prescher, G., Parker, S. F., and Ross, D. K., *J. Catal.* **181**, 145 (1999).
13. Renouprez, A. J., and Jobic, H., *J. Catal.* **113**, 509 (1988).
14. Giordano, N., Passalacqua, E., Pino, L., Arico, A. S., Antonucci, K., Vivaldi, M., and Kinoshita, K., *Electrochim. Acta* **36**, 1979 (1991).
15. Honji, A., Mori, T., and Hishinuma, Y., *J. Electrochem. Soc.* **137**, 2084 (1990).
16. Bowden, Z. A., Celli, M., Cilloco, F., Colognesi, D., Newport, R. J., Parker, S. F., Ricci, F. P., Rossi-Albertini, V., Sacchetti, F., Tomkinson, J., and Zoppi, M., *Physica B* **276–278**, 98 (2000).
17. Celli, M., Colognesi, D., and Zoppi, M., *Eur. Phys. J. B*, in press.
18. Mitchell, P. C. H., Parker, S. F., Tomkinson, J., and Thompsett, D., *J. Chem. Soc., Faraday Trans.* **94**, 1489 (1998).
19. Szilágyi, T., *J. Catal.* **121**, 223 (1990).
20. Parker, S. F., Coombs, D., and Chesters, M. A., unpublished results.
21. Nakamoto, K., "Infrared and Raman spectra of Inorganic and Coordination Compounds Part A: Theory and Application in Inorganic Chemistry," 5th ed., p. 140. Wiley, New York, 1997.
22. White, J. W., and Wright, C. J., *J. Chem. Soc., Faraday Trans. 2* **68**, 1423 (1972).
23. Chabal, Y. J., *J. Electron Spectrosc. Relat. Phenom.* **38**, 159 (1986).
24. Erskine, J. L., Woods, J. P., Kulkarni, A. D., and de Wette, F. W., *J. Electron Spectrosc. Relat. Phenom.* **44**, 27 (1987).
25. Zemyanov, D. Yu., Smirnov, M. Yu., and Gorodetskii, V. V., *Catal. Lett.* **43**, 181 (1997).
26. Baró, A. M., Ibach, H., and Bruckmann, H. D., *Surf. Sci.* **88**, 384 (1979).
27. Richter, L. J., and Ho, W., *Phys. Rev. B* **36**, 9797 (1987).
28. Koelman, B. J. J., de Zwart, S. T., Boers, A. L., Poelsma, B., and Verheij, L. K., *Phys. Rev. Lett.* **56**, 1152 (1986).
29. Reutt, J. E., Chabal, Y. J., and Christman, S. B., *J. Vac. Sci. Technol. A* **6**, 816 (1988).
30. Feibelman, P. J., and Hamann, D. R., *Surf. Sci.* **182**, 411 (1987).
31. Olsen, R. A., Kroes, G. J., and Barends, E. J., *J. Chem. Phys.* **111**, 11155 (1999).
32. Richter, L. J., Germer, T. A., Sethna, J. P., and Ho, W., *Phys. Rev. B* **38**, 10403 (1988).
33. Conrad, H., Kordesch, M. E., Stenzel, W., Šunjić, M., and Trninic-Radja, B., *Surf. Sci.* **178**, 578 (1986).
34. Wilson, Jr., E. B., Decius, J. C., and Cross, P. C., "Molecular Vibrations." Dover, New York, 1955.
35. Kearley, G. J., *Nucl. Instrum. Methods Phys. Res. A* **354**, 53 (1995).
36. Ross, D. K., "Hydrogen in Metals III: Properties and Applications" (H. Wipf, Ed.), Topics in Applied Physics, Vol. 73, p. 153. Springer-Verlag, Berlin, 1997.
37. Rush, J. J., Cavanagh, R. R., Kelley, R. D., and Rowe, J. M., *J. Chem. Phys.* **83**, 5339 (1985).
38. Chesters, M. A., Packer, K. J., Lennon, D., and Viner, H. E., *J. Chem. Soc., Faraday Trans.* **91**, 2191 (1995).